3.0 SUMMARY

In this section some of the scientifically and technologically important conclusions of the work are summarized. These include the performance of the newly developed catalyst, the relationship between properties and function of ruthenium catalysts, the investigation of hydrocarbon cutoff hypothesis, characterization of coke on used ruthenium catalysts, and the role of the new modifier.

3.1 Newly Developed Catalyst

3.1.1 Current Performance

A new stable Fischer-Tropsch catalyst with very high selectivity to distillate fuels and with low light ends production was developed. This catalyst, made by a reverse micelle technique, contains 2.8% (by weight) ruthenium in the form of 4-6 nm particles on alumina and a proprietary modifier. A patent application has been made for this catalyst.

The new modified ruthenium catalyst did not noticeably deactivate during 814 hours at about 80% CO conversion, $2H_2$:1 CO feed ratio, 208°C at inlet, 62 atm and 150 gas hourly space velocity. In order to determine the catalyst's tolerance, the operational severity was increased between 814 hours and 1700 hours by increasing in parallel the temperature and space velocity to 225°C at inlet and to 205 hr^{-1}, respectively. A deactivation rate of about 0.016%/hour was measured under these more severe conditions at about 70% conversion level.

Deactivation of the new modified ruthenium catalyst seems to have occurred by migration of ruthenium particles to the exterior of alumina particles followed by agglomeration. The causes for the migration of ruthenium particles are not known but appear to be related to filling of the alumina pores with Fischer-

Tropsch products. On the other hand, unmodified ruthenium catalysts deactivated by coking and not by agglomeration.

A total of 787 g hydrocarbons + oxygenates was made with 0.15 g ruthenium in this catalyst during this 1700-hour-demonstration run. Approximately 55% of the products were in the distillate range (C_5-C_{22}) for both test periods. The light ends (C_1-C_4) amounted to 9.5% of the total products made during the first 814 hours. Since the light ends selectivities gradually decreased during the first 500 hours on stream, the lined-out light ends production is much lower than the average value reported here. The light ends selectivity was higher (13%) during the second test period because of the higher temperature and lower conversion level. The balance of the products was wax, which could be efficiently hydrocracked to make more distillates.

These results with the new modified ruthenium catalyst compare favorably with those reported for the two commercial Sasol processes. The Arge process makes approximately 38% distillate fuel with no less than 18% light ends, while the Synthol process makes about 48% distillate with 38% light ends.

The Anderson-Schulz-Flory product distribution exhibited a maximum at a carbon number of about 15. This maximum was reproducible in three other tests conducted with ruthenium catalysts at 62 atm, but was not observed at 35 atm tests. The data analysis method contributes to determination of the maximum in the Flory distribution. In contrast to C_5-C_{10} data, the C_{10}+ carbon number products were calculated based on the boiling point of the n-paraffin from the chromatographic distillation measurements. However, the distillate range products contained about 20% alcohols + aldehydes, which were lumped together during chromatography with the n-paraffins having -2 higher carbon numbers. This maximum in the Anderson-Schulz-Flory distribution becomes less significant when the oxygenates are plotted at their correct carbon numbers and/or if the oxygenates are not included in the Anderson-Schulz-Flory distribution.

While the specific activity (per weight of catalyst) of the 170-200 mesh ruthenium catalyst may be comparable to the Arge iron catalyst's reported activity, on a catalyst volume basis the ruthenium catalyst was less active. Specifically, the Arge catalyst can achieve ~80% conversion at about 700 gas hourly space velocity, at 225°C and 45 atm [34]. This indicates that, on a catalyst volume basis, it is 3-4 times more active than the new modified ruthenium catalyst. This difference is mostly arising from the density difference between the iron catalyst and the alumina support that was used for the ruthenium catalyst.

3.1.2 Potential for Improvement of the New Catalyst

3.1.2.1 Effect of Modifier

The proprietary modifier used in this work attenuated 50% of ruthenium's initial activity, and 50% additional activity loss was observed during the first 20 hours. Therefore, a more suitable concentration of modifier or a different modifier may result in as much as 400% increase in ruthenium specific activity.

3.1.2.2 Effect of Metal-Support Interacation

This work also indicated that a minimum of 4 nm size was necessary on alumina in order to maintain the ruthenium particle size during Fischer-Tropsch synthesis. The ruthenium particle size with the modified catalyst was mostly 4-6 nm with some 10-20% of the ruthenium in the 3-4 nm and 6-40 nm size range. Since a 5 nm ruthenium has approximately only 30% of the ruthenium atoms on the surface of the particles, with the modified catalyst no more than 1 out of 3 to 4 ruthenium atoms were being effectively utilized. However, the turnover number for these relatively large particles on alumina are typically much higher than that for highly dispersed ruthenium.

On TiO_2 and Y-type zeolite much smaller ruthenium particles were able to maintain their size during the Fischer-Tropsch synthesis, but large amounts of methane + ethane were formed, as was observed on alumina.

Past work indicates that metal particle size and metal-support interaction play a key role in influencing activity, selectivity and maintenance of catalyst form during Fischer -Tropsch synthesis. The optimal ruthenium particle size, of about 4 nm on alumina, may be much smaller on other supports. Since no more than 1 out of 3 to 4 ruthenium atoms are being effectively utilized in the modified catalyst prepared on alumina, a more suitable support on which highly dispersed ruthenium performs satisfactorily may result in as much as 300-400% additional increase in ruthenium specific activity.

3.1.2.3 Effect of a Second Bimetallic Component

Recent work conducted at Exxon indicated an apparent synergism between ruthenium and cobalt which was present as a second bimetallic component in the catalyst [81]. A 300% improvement in activity was achieved when 0.14% Ru was added to 11.6% Co catalyst on TiO_2. The activity of Ru-Co catalyst appeared to exceed that of the ruthenium-only and cobalt-only catalysts. Consistent results were obtained at Gulf with 20% Co + $La_2O_3/\gamma Al_2O_3$ catalysts promoted with 0.1-0.5% Ru [82].

3.1.2.4 Strategy for Spent Catalyst

The modifier in the new catalyst apparently increased catalytic stability of ruthenium but also changed the deactivation mechanism. The deactivation was by agglomeration of ruthenium. There is no established procedure for redispersing 15-25 nm ruthenium particles in the used catalyst to the 4-6 nm size range that prevailed in the fresh catalyst. In used supported catalysts with agglomerated noble metal, chloride treatment totally redisperses the noble metal.

This would result in a ruthenium particle size which is too small for Fischer-Tropsch. Threrfore, a ruthenium catalyst which has extensively agglomerated may not be easily regeneratable. However, ruthenium is expected to be recovered with a high efficiency from the spent catalyst.

3.1.2.5 Overall Assessment

The discussion in Sections 3.1.2.1-3.1.2.3 indicates that there is potential for increasing the specific activity of ruthenium substantially by a suitable choice of the modifier, support, modifier level, ruthenium particle size and possibly by the presence of a second bimetallic component. Accordingly, the ruthenium metal loading on the catalyst may be reduced while still delivering high converison at a high space volocity. Furthermore, it is conceivable that optimization of the modifier may result in minimization of ruthenium metal agglomeration. If the ruthenium agglomeration rate during Fischer-Tropsch synthesis is slow then the major deactivation pathway would be deposition of carbonaceous deposits. Then, the catalyst should be regenerable.

3.1.3 Acativatiaon and Start-up Procedure

The activation of the new ruthenium catalyst was conducted externally. The catalytic performance is very sensitive to the activation procedure.

The start-up procedure used in this work for the new catalyst is described in Section 4.4.6. With this catalyst, the test conditions were changed initially in the run to achieve a desired conversion level. The impact of the start-up procedure and of the initial condition changes on catalytic performance have not been investigated because of limitations of research funds.

3.1.4 Reproducibility of the New Cgtalyst

The catalytic properties of the new modified ruthenium catalyst have been reproduced in a second preparation, as discussed in Section 5.3.5.1.3. However, this second catalyst has not been tested to check reproducibility of catalytic performance becasue additional research funds were not available.

3.2 Elucidating the Relationship Between Properties and Function of Ruthenium Catalysts

The relationship of ruthenium particle size and ruthenium-support interaction to activity, selectivity and stability against ruthenium agglomeration in Fischer-Tropsch synthesis was elucidated.

CO underwent three different types of reaction during Fischer-Tropsch synthesis with supported ruthenium catalysts:

1. CO can react with Ru to form ruthenium carbonyl.
2. CO can react with H_2 to make hydrocarbons + alcohols + aldehydes and H_2O.
3. CO can react with H_2O to form H_2.

The selectivity for each of these reactions, as well as hydrocarbon synthesis activity and chain growth probability in hydrocarbon synthesis varied with metal particle size in the fresh alumina-supported catalysts.

3.2.1 Ruthenium Metal Agglomeration

Ruthenium metal particles smaller than 4 nm agglomerated on Al_2O_3 via the formation of the volatile ruthenium carbonyl species. Ruthenium particles that were 4 nm or larger did not agglomerate. This effect may be explained by the

difficulty of dissociating CO over small ruthenium particles since ruthenium carbonyl formation requires undissociated CO.

Highly dispersed ruthenium did not agglomerate on Y-zeolite or on titania.

The causes for the enhanced stability of ruthenium in Y-zeolite relative to alumina may be explained by a possible cage effect exerted by the zeolite, although the evidence that ruthenium was inside the zeolite was not conclusive.

The causes for the enhanced stability of ruthenium on titania relative to ruthenium on alumina may be explained by a stronger ruthenium-support interaction in the case of titania. The SMSI (strong metal support interaction) effect with titania-supported ruthenium is supported by the low hydrogen uptake over ruthenium.

3.2.2 Water Gas Shift Reaction

Analysis, in the appendix, of the CO/H_2 reaction system in this work indicates that the water gas shift reaction and not the Boudouard reaction ($2CO \rightarrow CO_2+C$) was likely to be the source of CO_2. Accordingly, CO_2 formation, throughout this work, was tentatively attributed to the water gas shift reaction.

Water gas shift reaction during Fischer-Tropsch synthesis for unmodified alumina-supported catalysts was apparently only catalyzed by highly dispersed ruthenium. It was postulated that part of the highly dispersed ruthenium was in a positive oxidation state during Fischer-Tropsch synthesis, which may explain the occurrence of the water gas shift reaction.

Water gas shift activity of highly dispersed ruthenium catalyst apparently decreased with time, which was explained by agglomeration of ruthenium during Fischer-Tropsch synthesis.

Water gas shift reaction was not catalyzed by highly dispersed ruthenium on titania.

3.2.3 Hydrocarbon Synthesis Activity

The turnover frequency for hydrocarbon synthesis increased with the ruthenium particle size in the range of 0.8 nm to ~5 nm on alumina. This phenomenon has been previously documented in the literature. Activity is lower with smaller ruthenium particles probably because the probability of finding an ensemble of vacant metal atoms for dissociating the CO molecule decreases with decreasing ruthenium particle size.

3.2.4 Olefin-to-Paraffin Ratio

In situ production of H_2 through the water gas shift reaction was partly responsible for the low selectivity to olefinic products observed with highly dispersed ruthenium on alumina. In the absence of any significant water gas shift activity and at the same converison level, the propylene:propane ratios were still lower with smaller ruthenium particles on alumina, while butylene: butane ratios were similar. However, comparison of catalysts with different activity at the same temperature and conversion level necessitated the use of different space velocities, which may also influence the olefin to paraffin ratios. Accordingly, with alumina-supported catalysts definite conclusions on the effect of ruthenium particle size on the olefin to paraffin ratio cannot be reached.

Highly dispersed ruthenium did not exhibit water gas shift activity on titania and made products that were more olefinic. These results are, therefore, consistent with the interpretation given for alumina-supported catalysts.

3.2.5 Chain Growth Probability

Chain growth probability, like the turnover frequency for hydrocarbon synthesis, increased with the ruthenium particle size. This concurrent increase may be explained if the overall rate is controlled either by CO dissociation or by chain growth, both of which are likely to require a large ensemble of atoms.

3.2.6 General Applicability of Catalyst Preparation and Characterization Methods

The metal particle size control method used in this work, via reverse micelles, in principle, is applicable to supported cobalt catalysts. However, a suitable support material and a suitable metal particle have to be identified which would result in a desired level of cobalt-support interaction. The reverse micelle method is expected not to be applicable to iron catalysts, whic are either unsupported or have a too high metal loading on the support. The catalyst characterization methods employed in this work are applicable to the study of cobalt and iron catalysts.

3.3 Hydrocarbon Cutoff Hypothesis

The product distributions were Anderson-Schulz-Flory with increasing chain growth probability at higher carbon numbers and with no cutoff, at least up to C_{160}, with $\leq$2-4 nm ruthenium particles on alumina in Run 20, with smaller than 20Å ruthenium particles on titania in Run 30 and with 1.5 nm ruthenium particles on Y-zeolite in Run 28. These results indicate that cutoff was not affected by limiting the size of the active metal particle to the range investigated in this work.

It is conceivable that a very large number of literature reports of hydrocarbon cutoff are not valid, since these reports don't mention analysis of used catalysts for condensed hydrocarbons.

3.4. Characterization of Coke on Ruthenium Catalysts

After Soxhlet extraction by cyclohexane and toluene of the overwhelming majority of Fischer-Tropsch wax, the used catalysts showed, by XPS, two types of carbon with different chemistry. The majority of the carbon on the surface was hydrocarbon-like, while the other type appeared to be bonded to oxygen. This second type of carbon may be part of an oxygenate or may be carbon bound to the oxygen of the support.

Further Soxhlet extraction of the used catalyst with methylene chloride/methanol resulted in a decrease of both types of carbon on the surface, according to XPS measurements. HRMS, IR and fluorescence analyses of this final extract material showed three types of carbon compounds.

Part of the extract contained long chain olefinic or cyclic oxygenates that appeared to be acids and/or esters with carbon numbers up to 35. This result is consistent with XPS measurements, which indicated that a carbon apparently bound to oxygen was removed during the final extraction and, furthermore, suggests that part of the oxygen-bound carbon detected by XPS may be part of an oxygenate and not carbon bound to the oxygen of the support.

The second type of carbon was in the final extracts as paraffinic hydrocarbons, which typically makes up the Fischer-Tropsch wax. This result is also consistent with XPS measurements, which indicated that carbon in a hydrocarbon-type environment was removed during the final extraction.

The third type of detected carbon compound, which amounted to the minor material in the extracts, was aromatic and consisted of aromatic hydrocarbons, aromatic oxygenates and polynuclear aromatics. These paraffinic and aromatic hydrocarbons would not be easily distinguished from each other by XPS and are possibly related to the hydrocarbon-like carbon detected by XPS.

Examination of the alkylbenzene distribution in the extracts indicated that the aromatization tendency of Fischer-Tropsch olefins and/or paraffins increased with carbon number. It was also determined that the formation of polynuclear aromatics from alkylbenzenes was very favorable.

Aromatics amounted to the minor material in the extracts. However, aromatics may be harder to remove with the extraction techniques used here and, therefore, may be present at a relatively higher concentration on the catalyst surface.

NMR could not detect the carbon bound to oxygen. However, NMR detected two types of carbon with similar chemistry but with different mobility. The mobile carbon species had the same features as Fischer-Tropsch wax. This carbon could be a small portion of the wax retained in the used catalyst despite the Soxhlet extraction steps and is not expected to be chemically bound to the catalyst surface. The carbon with higher restriction to motion is possibly chemically bound to the catalyst surface. Alternatively, the 2 ppm NMR shift observed between the two carbon species may be caused by different restrictions for motion of wax-type hydrocarbons inside or outside the catalyst pores. However, the immobile carbon could also be removed during Soxhlet extraction with methylene chloride/methanol and, therefore, should be one of the three compounds detected in the final extracts.

According to results reported by A. Bell's group, α-type carbidic carbon connected to ruthenium and β-type carbon bound to ruthenium with a methylene group had about 7 ppm shift from each other in the NMR spectra. The observed 2 ppm shift in NMR spectra is probably not caused by the presence of α-type and β-type carbon on the catalyst.

The presence of multiple types of carbon on the used catalysts after Soxhlet extraction with cyclohexane was also confirmed by differential scanning

calorimetry (DSC) measurements. According to DSC measurements, two types of carbon were present, which burned at ~30°C different temperatures. Extraction with toluene and with methylene chloride/methanol resulted essentially in the disappearance of the low temperature peak and shifted the high temperature peak to lower temperatures.

3.5 Elucidation of the Role of Modifier in the Improved Catalytic Stability Observed

At least three criteria are needed for stable catalyst performance:

1. The catalyst must not lose metal surface area by agglomeration.

2. The coverage of active sites by the active carbon species should not indefinitely increase. This carbon species may form via CO dissociation on vacant active sites. This, then, implies that catalytic stability may be improved when the catalyst is modified in a manner that balances the CO dissociation rate relative to the hydrogenation rate of this active carbon into methyl and methylene species.

3. The hydrocarbons on the surface should not be converted into polynuclear aromatic (PNA) compounds which are precursors for graphitic carbon. Therefore, a modifier which suppresses the dehydrogenation/cyclization reaction of hydrocarbons into PNA's may improve catalytic stability.

The extent of ruthenium metal surface area loss through agglomeration observed at the end of Run 46 with the new modified ruthenium catalyst can

explain the observed deactivation. This may indicate that, for this catalyst, deactivation by coking is minimal. These results are in sharp contrast to those observed with unmodified ruthenium catalysts. One such an example is the unmodified ruthenium Catalyst 4966-198. This catalyst gradually deactivated during Run 47 although the ruthenium particle size remained 4-6 nm during the 825-hour run, indicating that deactivation probably was via coking.

Examination of used catalysts indicates that the amount of coke on the modified catalyst was much less than the amount on the unmodified catalyst, although the test with the modified catalyst was 886 hours longer. The modified ruthenium catalyst showed a lesser amount of hydrocarbon-type carbon and carbon associated with oxygen, according to XPS. A carbon with restricted motion was also present in lesser quantities on the modified catalyst. Finally, low quantities of aromatics and no polynuclear aromatics were detected, which are in sharp contrast to results obtained with unmodified ruthenium catalysts.

These results indicate that the modifier may have improved catalytic stability by controlling the surface concentration of the active carbon species. This may have been possible if attenuation of ruthenium's initial activity was caused by a decrease in the rate of CO dissociation. A slower rate of formation of the active carbon species may then be more easily balanced by the hydrogenation rate of this carbon species.

It is important to note that there was an apparent inverse correlation between ruthenium's initial activity and the binding energy of ruthenium's $3p_{3/2}$ electrons, as determined by XPS. The ruthenium's binding energy appeared to increase with modification of ruthenium, which also resulted in attenuation of ruthenium's initial activity. For example, iridium appeared to increase ruthenium's binding energy to a greater extent than the proprietary modifier identified in this work, and also caused more attenuation of initial activity.

However, binding energy differences between modified and unmodified catalysts were small, and, therefore, definite conclusions are not possible.

Alternatively, the modifier may have improved catalytic stability by preventing the transformation of the active carbon species into polynuclear aromatic compounds via dehydrogenation/cyclization reactions.

It is not presently clear whether the alternative deactivation pathway observed with the modified ruthenium catalyst is directly caused by the modifier or is the result of the relatively severe operating conditions that prevailed during the second part of the test with the modified catalyst and, thus, would have occurred also with the unmodified catalyst.

4. EXPERIMENTAL

The experimental work in this report is described in six major sections. First, the pretreatment procedure for the reference iron catalyst C-73-1-101 will be described, followed by a description of reverse micelle and catalyst characterization techniques, description of the catalyst testing plant and procedure and finally description of product and run analyses procedures.

4.1 Pretreatment Procedure for the C-73-1-101 Iron Reference Catalyst

C-73-1-101 iron catalyst (a typical composition as reported by G. A. Huff [64] is shown in Table 4-1) from United Catalyst Inc. (sample number 3067-5) was crushed from 6-10 mm size range to smaller particles (greater than 100 mesh). A 228.9 g sample of this catalyst, which had a volume of 102 cc when loosely packed, was transferred to a 1 inch ID x 40 inch long quartz tube, which was then placed in an electric furnace. H_2 flow (Matheson zero gas, 99.99%) was initiated at 10 liters/min., resulting in a space velocity of 6000 hr^{-1} GHSV. Catalyst temperature was then raised to 450°C at 5°C/min. under hydrogen flow and maintained for 48 hours. The progress of catalyst reduction was monitored by discoloration of a drierite bed at the outlet of the catalyst. No further discoloration occurred at the end of 48 hours. The catalyst was then cooled to room temperature under hydrogen and then flushed with nitrogen before unloading. The catalyst was unloaded inside a nitrogen glove bag and its apparent bulk density was measured to be 2.14 g/cc. The catalyst was then transferred in the glove bag to a series of glass vials and sealed for further use.

Table 4-1

Typical Properties of C-73 Ammonia Synthesis Catalyst

Chemical Analyses (wt.% and dry basis):

FeO	30-37
Fe_2O_3	65-58
Free Fe	<0.5
Total Fe	67-69
Al_2O_3	2.0-3.0
K_2O	0.5-0.8
CaO	0.7-1.2
SiO_2	<0.4
P	<0.015
S	<0.001
Cl	<0.002
Fe^{2+}/Fe^{3+}	0.05-0.7

Physical Characteristics

Bulk density, g/cc 2.9 ± 0.15

Huff, G. A., Ph.D. Thesis, Massachusetts Institute of Technology, 1982 [64].

4.2 SAXS Procedure for Characterizing Micelle Solutions

Small angle x-ray scattering (SAXS) was used for characterizing the reverse micelle solutions used in the preparation of ruthenium catalysts. SAXS occurs because of the difference in electron density between the water core of the reverse micelles and the organic phase (surfactant plus organic solvent).

The radius of gyration of the water core of the reverse micelles, R_G, is determined from the scattering at very low angles, in the so-called Guinier region. R_G is determined from a plot of ln I vs. h^2, where I is the scattered intensity, $h = 4\pi\sin\theta/\lambda$, θ is one-half the scattering angle, and λ is the x-ray wavelength in Angstroms. This plot is linear in the Guinier region and its slope is equal to $-R_G^{2/3}$. For a single particle or for a monodisperse system, $R_G = 3r/5$. For a polydisperse system, R_G becomes the volume averaged radius of gyration. The diameter distributions were calculated by an algorithm developed by Vonk [65]. It was assumed here that the reverse micelles were spherical in shape.

4.3 Catalyst Characterization Techniques

Various techniques were utilized in order to characterize ruthenium's catalytic properties and the nature of coke deposited during Fischer-Tropsch synthesis.

H_2-titration of oxygen chemisorbed on ruthenium was used as a means of determining the relative ruthenium surface area for catalysts with different dispersions. H_2-titration experiments were useful for determining the relative average ruthenium particle size but may be misleading in cases where the ruthenium metal particle size distribution was wide. Another limitation for this kind of experiment is the difficulty of characterizing the metal particle size on used catalysts because of interference from coke. Because of these

limitations, the scanning transmission electron microscope (STEM) was extensively used to determine the size distribution for ruthenium particles larger than 2 nm on both fresh and used catalysts. Since, for metal oxide supported catalysts, STEM cannot usually detect metal particles smaller than 2 nm, selected catalysts with smaller ruthenium particles were examined by extended x-ray absorption fine structure (EXAFS).

X-ray diffraction (XRD) was used to measure the crystallite size distribution of the reduced C-73-1-101 iron reference catalyst. The same technique was also investigated for ruthenium catalysts.

Ruthenium electronic states were characterized by x-ray photoelectron spectroscopy (XPS), EXAFS and CO fourier transform infrared spectroscopy (FTIR). Ruthenium local coordination environments were characterized by EXAFS and STEM.

In an attempt to characterize the nature of coke, retained products were first removed from the used ruthenium catalysts by Soxhlet extractions with different solvents and then analyzed. Cyclohexane solvent removed most of the Fischer-Tropsch wax. More wax and some of the organic compounds with low polarity were removed by toluene. Finally, the more polar compounds were removed by a mixture of methylene chloride and methanol solvents (9:1 by wt.).

The extracts from Run 39 were analyzed by infrared spectroscopy (IR) and high resolution mass spectroscopy (HRMS). The methylene chloride/methanol extracts from Runs 46 and 47 were analyzed by IR, x-ray fluorescence and HRMS.

After the extraction, the extract solutions became supersaturated with wax at room temperature. All of the extract solutions contained insoluble wax particles. These particles were left in the extracts from Run 39. However, because they would interfere with the fluorescence analysis, they were removed from the Run 46 and Run 47 extracts, by decanting.

The solvents were removed completely from the Run 39 extracts with a stream of nitrogen gas and the residues were analyzed. The volume of extracts from Run 46 and Run 47 were both reduced from 300 to 5 milliliters with a nitrogen gas stream and the fluorescence spectrum obtained by the method described below. The volume of both of the extracts was reduced to the same amount so that the relative concentration of polynuclear aromatics in the extracts could be compared. The remaining solvent was then removed and the mass spectral data obtained.

The used catalysts from Runs 39, 46 and 47 were also analyzed by nuclear magnetic resonance spectroscopy (NMR), x-ray photoelectron spectroscopy (XPS), differential scanning calorimetry (DSC) and thermogravimetric analysis (TGA) after different Soxhlet extraction steps.

4.3.1 Gas Adsorption

Catalysts were reduced with UHP (ultrahigh purity) H_2 at 350°C for 1 hour, purged with an oxygen-scrubbed UHP helium for 15 minutes at 350°C and then cooled to room temperature in helium. Pulses of oxygen were then introduced over the catalyst and the amount of uptake was determined. The catalyst was then heated in helium to 50°C. Pulses of H_2 were then introduced over the catalyst. Chemisorbed oxygen was typically unreactive at 50°C and accordingly, the amount of H_2 uptake was low. The catalyst was then heated in helium to 375-380°C and further pulsed with H_2. Most of the H_2 uptake occurred under these conditions. The additional H_2 uptake at 500°C was relatively low (Figure 4-1). The total H_2 uptake was then taken to be proportional to the ruthenium surface area, i.e., it was assumed that all of the H_2 reacted with oxygen chemisorbed on ruthenium.

Figure 4-1

PROCEDURE FOR DETERMINING RELATIVE RUTHENIUM SURFACE AREA BY H_2 TITRATION MEASUREMENTS

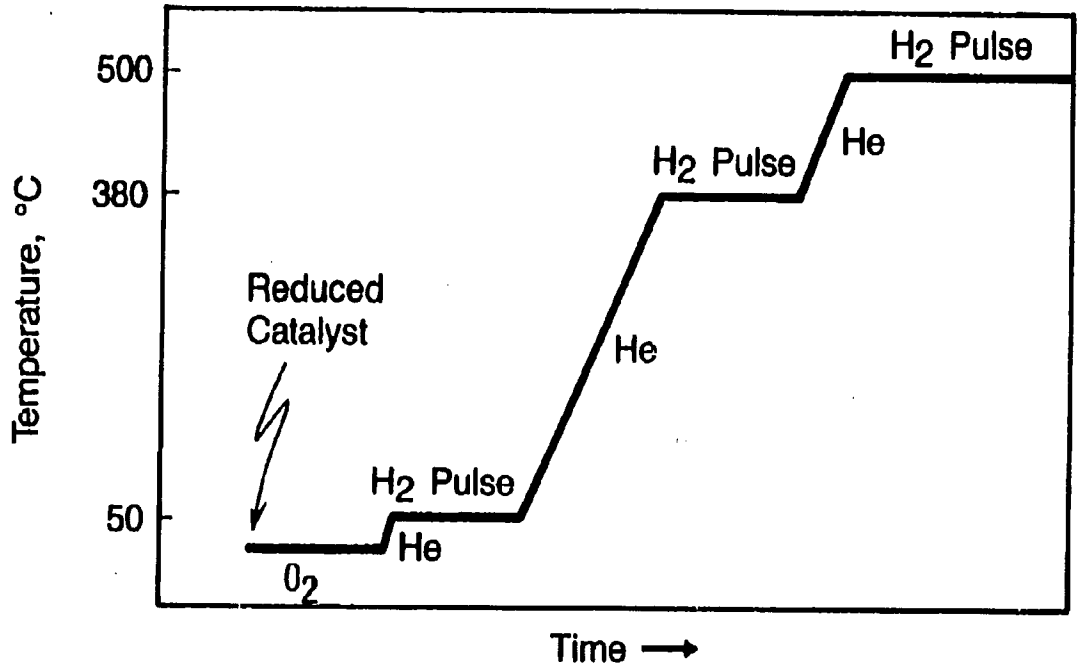

Possible Reaction: $RuO + H_2 \longrightarrow Ru + H_2O$

$Ru + H_2 \not\longrightarrow$

4.3.2 STEM

The STEM combines the best features of both the SEM (scanning electron microscope) and TEM (transmission electron microscope). The instrument has a cold field emission source which is capable of delivering a high intensity electron beam 0.5 nm in diameter to the specimen area. The resulting x-rays, diffracted electrons, electron energy losses, and scattered and absorbed electrons provide elemental and morphological information about the specimen. The energy dispersive x-ray analyzer (EDS) provides elemental information at atomic numbers >12, with a detectability limit of about 30 atoms of Pt. Electron energy loss spectroscopy (EELS) technique is used to estimate specimen thickness. Micro area electron diffraction (MAED) provides structural information from areas as small as 3 nm in size.

The catalysts were ground to a fine powder with a mortar and pestle under a N_2 atmosphere. The powder was deposited on a holey carbon-coated nylon grid which was treated with a drop of isopropanol. The excess powder was removed from the grid by gentle tapping. While under N_2, the specimen was placed in the cartridge and then into the HB-5 STEM. This was accomplished by transfer of the specimen in a N_2-purged glove bag to the sample delivery chamber of the HB-5, which also is purged with N_2. After the transfer was completed, the top of the HB-5 delivery chamber was put in place and the sample evacuated to 10^{-9} torr.

STEM examination typically involves first visually scanning, at relatively low magnification, two to four thousand alumina particles to determine whether large ruthenium particles are present. The presence of large ruthenium particles indicates that the catalyst was not prepared correctly, and the examination is terminated after taking a few photo micrographs. If there are no large ruthenium particles, then higher magnifications of 200,000 to 1,000,000 are used for determining the approximate ruthenium particle size distribution for a few

hundred alumina particles. Finally, 3-5 representative alumina particles are selected for closer examination and photo micrographs are taken. If there are no visible ruthenium particles, then 20-30 alumina particles are chosen at random to analyze for ruthenium using the energy dispersive x-ray analyzer. The intensities of ruthenium signal from different alumina particles are then compared to determine the uniformity of the ruthenium particle size distribution.

4.3.3 EXAFS

EXAFS was mostly used to measure the particle size of catalysts with smaller than 2 nm ruthenium particles, too small to be detected by STEM. EXAFS is a method which allows one to probe the immediate atomic environment of a selected type of atomic species. Since there is no requirement of long-range order as in diffraction methods, it has found broad application in the study of catalysts comprised of small particles. The UOP Des Plaines Technical Center is a member of a Progress Research Team at the National Synchrotron Light Source on beam line X18-B at Brookhaven National Laboratory. This line is fully operational and has been used extensively for investigations of supported Ru, Pt, Pd and Rh catalysts.

Two series of EXAFS measurements were taken for particle size characterization. The first series was conducted at Cornell High Energy Synchrotron Source (CHESS). The ruthenium catalysts which were previously reduced were transferred to sample cells under N_2 in a glove bag. Transmission detection was used for these measurements. The ruthenium particle sizes were characterized by a multi-shell analysis of EXAFS data. The second series of measurements were taken at Brookhaven National Laboratory. For this work ruthenium catalysts were treated with H_2 at 380°C and transferred to Kapton-sealed copper cells under H_2 before the EXAFS measurements were made. Fluorescence detection rather than conven-

tional transmission was used due to Kapton monochromator irregularities which introduce distortions to the transmission spectra. Multiple scans were collected and summed. The average ruthenium metal particle size was determined from the coordination number to nearest neighbors.

In order to understand the physical basis of the particle size determination by EXAFS, consider the two dimensional representation in Figure 4-2. For every atom in a "particle," one can count the number of nearest neighbors (the coordination number) and average this over the total number of atoms in the particle. This value is then the average coordination number for the first shell for a particle of this size. Results in Figure 4-2 illustrate that the average coordination number is higher with a larger particle and that the maximum value is 6. A similar analysis can be done in three dimensions. Figure 4-3 shows the variation of the nearest-neighbor coordination number with Pt particle size which can serve as a prototype for analysis of data for Ru. The coordination number in this figure is referenced to the infinite bulk solid and, therefore, gives relative coordination numbers. Rounding of the exact calculation was done to produce a smooth plot. Even though the exact bond lengths and crystal structures for Ru and Pt are different, the general shape of the plot and the relative coordination number will be within the range of experimental error. From 0.5 to 3 nm, there is a rapid increase in the relative coordination number. For particle sizes larger than 4 nm, the coordination number has nearly converged to the bulk value and no size discrimination can be expected in this range. These, then, indicate that EXAFS is a viable method for measuring catalyst particle sizes between 0.5 nm and 3 nm.

In a separate series of experiments at Brookhaven National Laboratory, EXAFS was used for characterizing ruthenium's local coordination environment in a modified and unmodified ruthenium catalyst. In this series, the catalysts

Figure 4-2

Nearest-Neighbor Coordination Number for a Small and a Large Crystallite

Nearest Neighbor

Coordination Number

3.64

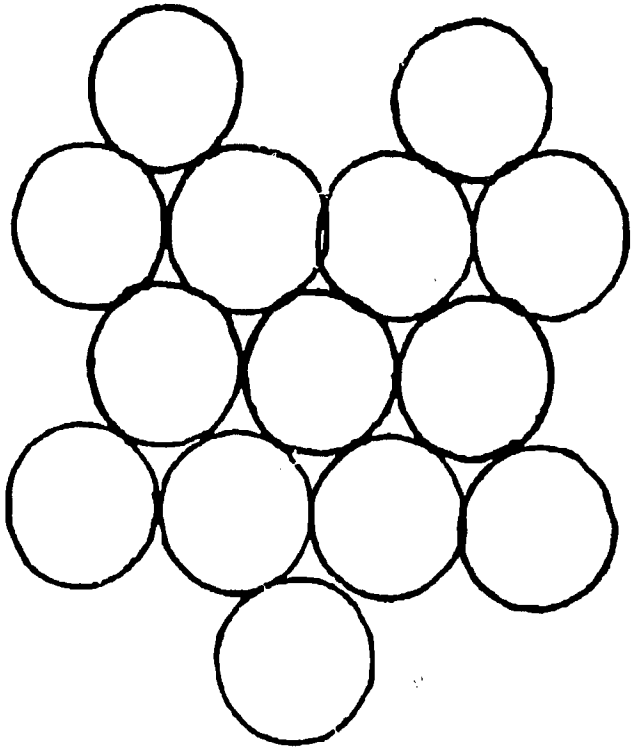

Small Crystallite

Nearest Neighbor

Coordination Number

5.11

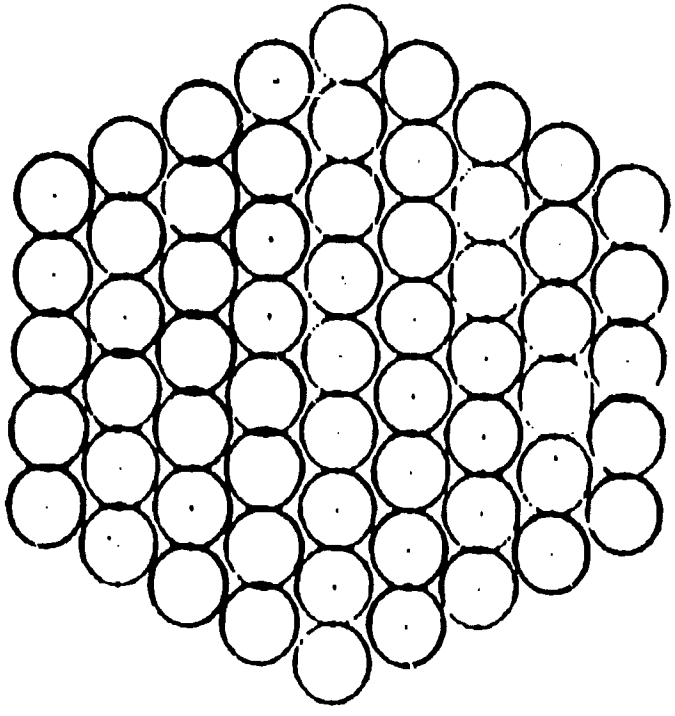

Larger Crystallite

Figure 4-3

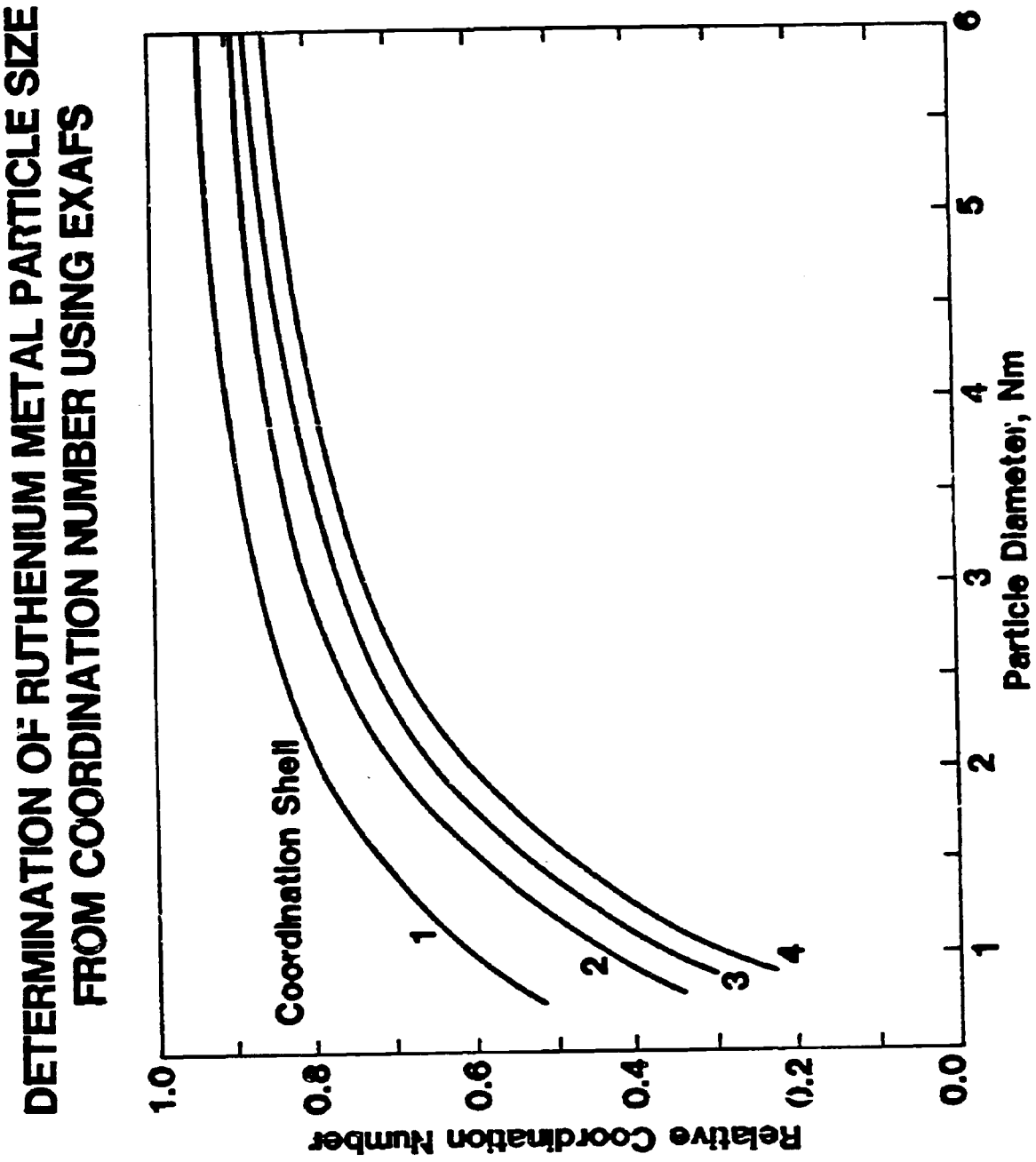
DETERMINATION OF RUTHENIUM METAL PARTICLE SIZE
FROM COORDINATION NUMBER USING EXAFS
Relative Coordination Number
1.0
0.8
0.6
0.4
0.2
0.0
Coordination Shell
1
2
3
4
1
2
3
4
5
6
Particle Diameter, Nm

were pressed into quartz tubes to give samples 3-4 mm thick. The samples were then loaded into the EXAFS reactor and treated in H_2 flowing at about 250 cc/min at 350°C for one hour. Following the 350°C treatment, the catalysts were cooled to about 100 K and the H_2 flow was reduced to about 10 cc/min to reduce the heat load on the catalysts. During the EXAFS measurements, the incident radiation was monochromatized using the CHESS channel-cut monochromator which utilizes a Si(220) crystal. The incident and transmitted beam intensities were monitored using gas filled ion chambers containing 0.2 atm Kr and 0.8 atm Kr, respectively. Each catalyst sample was scanned twice to assure data reproducibility.

4.3.4 XRD

A Philips wide angle diffractometer was used for measuring, by x-ray diffraction, the crystallite size distribution of reduced C-73-1-101 iron reference catalyst and two ruthenium catalysts. The data collection for this instrument is controlled by an automation package supplied by Nicolet. Data are transferred to a PDP 11/44 computer for analyses. The data collection is controlled by a multi-channel analyzer, while the analyses are done on the PDP 11/44 or IBM computer.

The measurements were done in a special cell which could be loaded in a controlled atmosphere enclosure to prevent oxidation of the catalyst. Two different window materials (Be metal and Kapton) were used in order to compare the results obtained with each.

For the reduced C-73-1-101 iron catalyst, the procedure consisted of very long time scans of two Fe reflections, the (200) and (211), in order to accurately determine the full lineshape and adjoining background. Similar scans were done for an Fe powder where the lineshape is essentially an instrument function. Then the Fe standard and Fe catalyst lineshapes were Fourier analyzed and the instrumental broadening was removed from the catalyst lineshape to yield the

true catalyst lineshape. The true lineshape is obtained as a Fourier series, which is the preferred form, as the amplitudes of the Fourier coefficients contain the information about the distribution of crystallite sizes.

By plotting the amplitude of the Fourier coefficients versus the harmonic number, the extrapolated initial slope yields the mean crystallite size as the intercept of the abscissa. The distribution of sizes is obtained as the curvature of this plot versus harmonic number. The curvature is determined by numerical techniques which result in a loss of information at small crystallite size. At large size, the noise due to small Fourier coefficient leads to unrealistic curvature, resulting in large, but unrealistic probabilities.

X-ray diffraction (XRD) measurements were also done on two ruthenium catalysts with ruthenium crystallites mostly in the 4 to 6 nm size range. The objective was to confirm the results obtained in the STEM examination and to obtain a statistically more reliable determination of the distribution of crystallite sizes. Measurements were also done on a ruthenium metal powder in order to identify the ruthenium peaks best suited for lineshape analysis.

4.3.5 XPS

XPS was used to detect potential contaminants for the ruthenium catalyst used in Run 26, to measure ruthenium's electronic properties in modified and unmodified ruthenium catalysts and to characterize the nature of carbon species on the surface of ruthenium catalysts used in Runs 39, 46 and 47.

In XPS experiments, x-rays are used for ejecting electrons from atoms in the catalyst. By scanning a range of electron energies, the binding energy of a specific electron in the sample can be determined. The ruthenium $3p_{3/2}$ electrons' binding energy is related to ruthenium's electron density. In the case of used catalysts, the binding energy of the carbon 1s electron was used to determine the nature of carbon species.

All measurements were done using a Hewlett Packard Model 5950 A ESCA spectrometer. A positive pressure nitrogen glove box surrounds the sample entry system of the spectrometer, thus permitting the transfer of catalysts with air sensitive surfaces directly from the reactor into the high vacuum of the instrument. Fresh reduced ruthenium catalysts (40-200 mesh) were rereduced *in situ* with 350 torr of H_2 at 200°C for 1 hour prior to the XPS measurements. One of the catalysts was analyzed without the *in situ* treatment to determine the effect of the H_2 treatment. Used catalysts were analyzed as-received.

All binding energies were referenced against an Al 2p energy = 74.40 eV determined from the measurements done with the alumina support used for preparing the ruthenium catalysts. The Al 2p energy in the experiment with the alumina support was determined by assigning the C 1s energy = 284.60 eV for the adventitious carbon detected on the alumina support. During these experiments, optimized flood gun settings were used to minimize charging.

4.3.6 CO FTIR

The stretching frequency of CO adsorbed on Ru was monitored by diffuse reflectance FT-IR spectrometry (DRIFT) and used to characterize ruthenium's electronic state. The DRIFT experiments were conducted with a Nicolet instrument using a 60SX mid-infrared spectrometer equipped with Nicolet 1280 microprocessor and Micro Vax II off-line spectral analysis capability. The 60SX spectrometer is a research grade instrument with resolution as high as 0.2 cm^{-1} and high throughput from 4000 to 400 cm^{-1}. The DRIFT environmental cell has high optical collection efficiency and allows *in situ* sample treatments. *In situ* sample treatments significantly improved spectral reproducibility without tedious re-aligning of the IR accessory, like in the cases of off-line sample treatments. Other existing accessories required attenuated total reflection

(ATR) and spectral reflectance are also very useful in sampling species adsorbed on catalysts. Both TGS and liquid nitrogen cooled MCT (mercury-cadmium-tellurium) detectors are available. The MCT detector has higher sensitivity which is particularly suitable for characterizing catalysts with low ruthenium loadings and supported on strong infrared absorbing material.

Ruthenium catalyst (0.25 g) was first loaded to the cell and purged with He for 30 minutes at room temperature. The catalyst temperature was then raised to 400°C under He flow. He flow was then replaced with H_2 flow at 400°C for 2 hours to reduce the oxidized ruthenium. At the end of 2 hours H_2 was replaced with He and the catalyst was cooled under He to room temperature. CO (25 ml) was then injected into the cell. Excess CO was removed from the system by passing He over the catalyst, and then the spectrum of adsorbed CO was recorded.

4.3.7 IR

Infrared spectroscopy was used to identify the functional groups that are present in solvent extract residues from used catalysts by the presence of certain characteristic absorbances in the spectrum.

IR data was taken by a Perkin-Elmer 580B spectrometer. Pre-calibration of the instrument was done with a polystyrene film to insure the frequency accuracy. Due to the physical nature of the samples, the extract residues could not be analyzed by using a standard IR cell. A thin film pressed between two KBr salt plates was made and scanned over the full absorbance range from 4000 cm^{-1} to 500 cm^{-1}.

4.3.8 Fluorescence

Fluorescence Spectroscopy was used to determine the presence of polynuclear aromatic hydrocarbons (PNA) in trace concentrations in the solvent extract

solutions from used catalysts. Fluorescent spectra are obtained by irradiating with a narrow-wavelength light band obtained either by a filter or by a monochromator. The peaks corresponding to PNA's are detected at wavelengths between 300-600 nm.

The 5 ml solvent extract solutions from Runs 46 and 47 were analyzed using the Perkin-Elmer Model MPF-44B fluorescence spectrometer. This unit is equipped with dual monochromators and dual scan control. Synchronous scanning fluorescence was used to obtain the spectra using 10 mm path length quartz cells. The following instrumental settings were used:

$\Delta\lambda$	6 nm
Monochromator Bandpass	3 nm
Dynode Voltage	-750 V @ 536 nm
Signal Gain	3-100 (as required)
Scan Rate	120 nm min^{-1}
Wavelength Range	280-520 nm
Time Constant	0.2 sec
Mode	Ratio, AC

4.3.9 HRMS

High resolution mass spectrometry was used to obtain information on the molecular mass and structure of organic compounds in solvent extracts from used catalysts. It permits the identification of oxygen-containing molecules, as well as hydrocarbon species by the accurate mass measurement of the peaks produced by ionization of the sample in the mass spectrometer. These peaks can be either molecular ions from which one can obtain the elemental formula of the compound or fragment ions which can provide information on the structure of the material. The aromatic hydrocarbons do not fragment during ionization process in the MS instrument and, therefore, produce intense molecular ion peaks, and these were

used to obtain a carbon number range for these compounds. Saturated hydrocarbons and oxygenated saturated compounds fragment easily and often do not give molecular ion peaks. These solvent extracts were mixtures containing primarily heteroatom species and hydrocarbons, which do not have strong molecular ion peaks. Therefore, emphasis was placed on studying the fragments and rearrangement ions present in the mass spectra. At the 6,500 mass resolution utilized, species containing one, two and three oxygen atoms per molecule can be separated from the hydrocarbon species containing only carbon and hydrogen up to a molecular weight of approximately 200. Most oxygenated compounds fragment easily and do not have large molecular ions. Therefore, their more intense fragment ions were detected in the mass spectrum. Data have been compiled in the literature on the characteristic fragmentation paths and rearrangement ions formed for various types of oxygenated compounds, and these data [66-68] were used to identify the oxygenated types present in the sample.

The mass spectrometer used was a Kratos MS-30. The Kratos instrument is equipped with a heated all-glass 1ℓ expansion sample reservoir operated at a vacuum of 10^{-4} torr and separated from the source by a molecular leak. Attached to the reservoir is a specially designed all-glass breakoff sampling system [69]. The all-glass design of this system minimizes thermal decomposition of samples. Instrument settings used in this work were:

Mass Range	750-50 AMU
Ion Accelerating Voltage	3,870 volts
Mass Resolution	6,500
Multiplier Voltage	3,000 volts
Scan Rate	100 sec decade^{-1}
Filament Ionizing Voltage	30.0 e.v.
Source Temperature	200°C
Sampling System Temperature	350°C
Sample Size	1/2 microliter

4.3.10 NMR

NMR was used for characterization of the chemical nature of carbon on used ruthenium catalysts in Runs 39, 46 and 47. NMR measures the spinning frequency of nuclei in a strong magnetic field. The technique is nuclei specific and, therefore, each element can be observed individually, although only selected isotopes and elements can be examined. C-13 is one of the most commonly observed elements. Individual resonances are observed for carbons in a variety of chemical environments, i.e., aromatic, methyl, methylene. The individual peaks are often resolved enough to make finer distinctions, i.e., between structurally unequivalent methylenes.

The major limitations are sensitivity, due to small energy differences measured by NMR, the low natural abundance of C-13 nuclei, and the presence of anisotropic and dipolar interactions which lead to severe peak broadening. The latter are averaged out for translationally mobile molecules in solution and waxes. For immobile species it is necessary to employ high powered cross polarization decoupling and high speed "magic angle" spinning (CP/MAS) to observe peaks.

Two separate experiments were performed for each used ruthenium catalyst. The first was a magic angle spinning experiment with high power decoupling. This experiment only allows observation of mobile species. In the absence of the catalyst all of the carbons in the wax would yield observable resonances. The magic angle spinning does yield some line narrowing for the waxes, but the major reason for spinning the samples was to improve comparisons with the second experiment. In the second experiment CP/MAS was used to observe both the mobile and immobile species simultaneously.

The carbon NMR spectra were obtained with a Chemagnetics CMC 100 NMR spectrometer at 25 MHz. Zirconia sample holders (295 mm) were used in con-

junction with a low carbon background probe. All samples were spun at 54.7 degrees at rates exceeding 3.3 kHz. A 5.1 μsec 90° pulse was used. Approximately 12,000-24,000 scans were acquired with a delay of 2 secs between scans. Cross polarization conditions were established using a sample of catalyst physically mixed with wax. The reflected power from the probe was less than 4%.

4.3.11 DSC

DSC and TGA measurements provided information on the burning characteristics of carbon retained on used ruthenium catalysts in Runs 39, 46 and 47. DSC measurements were done with a DuPont 9900 Thermal Analyzer.

In DSC experiments, the used ruthenium catalyst was heated from room temperature to 600°C at 5°C/min under air flow and the heat flow to or from the catalyst was measured. A minimum in the DSC curve indicates the occurrence of an endothermic reaction, i.e., water evolution from the catalyst. A maximum in the DSC curve indicates the occurrence of an exothermic reaction, i.e., burning of the coke. The position and magnitude of various DSC maxima were then related to the nature of coke.

4.3.12 TGA

TGA measurements were done with the same DuPont 990 Thermal Analyzer that was used for DSC measurements.

In TGA experiments the percent weight loss was measured as the catalyst was heated from room temperature to 600°C at 5°C/min under air flow. These measurements also provided the derivative of the catalyst weight loss with respect to time. TGA data were necessary for determining whether the DSC maxima were actually caused by the burning of coke and not by a phase transformation reaction which may be exothermic but would not result in weight loss.